frontiers | Frontiers in Marine Science

TYPE Original Research
PUBLISHED 15 August 2025
DOI 10.3389/fmars.2025.1654677

OPEN ACCESS

EDITED BY
Amit Ranjan,
Tamil Nadu Fisheries University, India

REVIEWED BY
Santhiyagu Prakash,
Tamil Nadu Fisheries University, India
Aron Santhosh kumar Yohannan,
National Institute of Ocean Technology, India

*CORRESPONDENCE
Chiquan He
cqhe@shu.edu.cn
Jinlin Liu
jlliu@tongji.edu.cn
Peimin He
pmhe@shou.edu.cn

RECEIVED 26 June 2025
ACCEPTED 25 July 2025
PUBLISHED 15 August 2025

CITATION
Liu W, Zhang M, Xiong X, He C, Liu J and He P (2025) Macroalga *Ulva prolifera* O.F. Müller: an efficient biofilter for nitrogen-enriched aquaculture effluents. *Front. Mar. Sci.* 12:1654677. doi: 10.3389/fmars.2025.1654677

Macroalga *Ulva prolifera* O.F. Müller: an efficient biofilter for nitrogen-enriched aquaculture effluents

Wei Liu[1], Meijing Zhang[2], Xian'an Xiong[1], Chiquan He[1*], Jinlin Liu[3*] and Peimin He[2*]

[1]School of Environmental and Chemical Engineering, Shanghai University, Shanghai, China, [2]College of Oceanography and Ecological Science, Shanghai Ocean University, Shanghai, China, [3]State Key Laboratory of Marine Geology, Tongji University, Shanghai, China

Introduction: *Ulva prolifera*, a dominant species in green tides, exhibits remarkable nitrogen absorption capacity, yet its kinetics as a biofilter in recirculating aquaculture systems (RAS) remain unquantified.
Methods: This study systematically characterized NH_4^+-N, NO_3^--N, and NO_2^--N uptake kinetics in nitrogen-starved (7-day). *U. prolifera* across eight concentration gradients (NH_4^+-N: 0.5–35 μmol·L^{-1}; NO_3^--N: 5–130 μmol·L^{-1}; NO_2^--N: 2.5–60 μmol·L^{-1}).
Result: Michaelis-Menten modeling revealed: NO_3^--N achieved the highest maximum uptake rate (V_{max} = 161.29 μmol·g^{-1}·h^{-1}), but the greatest half-saturation constant (K_m = 29.40 μmol·L^{-1}); NH_4^+-N showed the strongest affinity (K_m = 4.60 μmol·L^{-1}); NO_2^--N absorption plummeted at >50 μmol·L^{-1} (41% removal after 6h). When the initial concentrations were below 20 μmol·L^{-1} for NH_4^+-N, or below 90 μmol·L^{-1} NO_3^--N, or below 20 μmol·L^{-1} for NO_2^--N, 1 g of *Ulva prolifera* in 1 L of seawater completely achieving 100% removal efficiency for each within 6 hours. Critical inhibition thresholds were identified: NH_4^+-N >20 μmol·L^{-1} reduced removal by 40–60%, NO_3^--N >110 μmol·L^{-1} induced suppression, and NO_2^--N >30 μmol·L^{-1} triggered acute inhibition.
Conclusion: We propose optimized RAS protocols: maintain NH_4^+-N ≤20 μmol·L^{-1} and NO_2^--N ≤30 μmol·L^{-1}, with 1.5–2× increased algal biomass when high total inorganic nitrogen concentration to sustain >90% nitrogen removal. This work demonstrates *U. prolifera*'s nitrogen assimilation strategy—"high ammonium affinity, high nitrate capacity, nitrite sensitivity"—providing a mechanistic foundation for valorizing green-tide macroalgae in sustainable aquaculture.

KEYWORDS

RAS, *Ulva prolifera*, nitrogen absorption kinetics, eutrophication, biofilter, green tide

1 Introduction

Despite rising food production, global hunger persists, affecting over 700 million people in 2023 (FAO, 2024). Meeting growing food demand sustainably is a critical challenge (Ahmed et al., 2019). Aquaculture has become vital, providing essential high-quality protein and trace elements to meet population needs, especially as capture fisheries decline due to overfishing and pollution (Li et al., 2023; Yan et al., 2021). Marine resources provide more extensive space, lower carbon footprints, stronger water currents, and faster pollutant dispersion than freshwater systems. With these advantages and the higher added value of marine aquaculture products, this sector has emerged as the dominant source of aquatic products (Shen et al., 2024). However, intensified high-density practices, while productive, cause significant environmental impacts through extensive methods and poor feed management (Verdegem, 2013). China is a major aquaculture country, with its aquaculture output accounting for more than half of the global total, a trend that has raised concerns about water environmental safety (FAO, 2019). In fact, between 2006 and 2017, as China fish and shellfish production increased from 30 to 47 million tons (Mt), nitrogen (N) releases rose from 1.0 to 1.6 Mt/year, while phosphorus (P) releases increased from 0.1 to 0.2 Mt/year (Ahmed et al., 2019). The level of eutrophication in the coastal waters is gradually increasing, accompanied by algal blooms such as “red tides”, “brown tides”, “green tides” and “golden tide” (Kong et al., 2012; Song et al., 2022; Sun et al., 2024; Zhang et al., 2019). In conclusion, achieving sustainable expansion of aquaculture operations while ensuring environmentally friendly practices has emerged as a critical contemporary priority.

Intensive aquaculture operations currently require substantial inputs of chemical supplements such as feed and fertilizers. These substances are not fully utilized by farmed organisms, while metabolic processes of organisms generate additional waste, collectively contributing to environmental impacts (Turcios and Papenbrock, 2014). Aquaculture effluent contains elevated nitrogen and phosphorus concentrations that drive eutrophication and promote harmful algal blooms (Sun et al., 2024; Wang et al., 2018, Wang et al., 2020). Recently, recirculating aquaculture systems (RAS) have emerged as a validated solution for effective wastewater treatment (Cahill et al., 2010; van Rijn, 2013). Crucially, RAS operates independently of natural environmental constraints, enabling the cultivation of diverse species irrespective of their native distribution or habitat requirements (Ahmed and Turchini, 2021; Dalsgaard et al., 2013). However, the accumulation of nitrogenous waste represents a critical constraint affecting the sustained operation of RAS. Such waste primarily comprises nitrate, nitrite, and ammonium nitrogen (Nelson et al., 2001). Notably, ammonium nitrogen exhibits both acute and chronic toxicity to aquatic species and constitutes a primary constraint on system functionality (Cahill et al., 2010; Randall and Tsui, 2002). Implementing effective filtration or purification methods is therefore essential for ensuring the long-term viability of RAS. Macroalgae are proposed as biofilters in RAS due to their superior nitrogen uptake efficiency compared to conventional filter membranes (Mangott et al., 2020), while offering significant potential for carbon dioxide sequestration to support climate change mitigation (Ahmed and Turchini, 2021; Goddek et al., 2015). In addition, cultivated macroalgae in RAS can be harvested as valuable aquaculture products (e.g., food or bioresources), thereby improving overall RAS profitability.

Macroalgae perform well in the process of aquaculture wastewater treatment, especially species of *Ulva* and *Gracilaria*, which are the most commonly used genera in RAS biological filtration (Lavania-Baloo et al., 2014). Specific species such as *Ulva lactuca*, *Ulva rigida*, *Ulva fasciata*, *Gracilaria conferta*, *Gracilaria vermiculophylla*, *Gracilaria chilensis*, *Gracilaria bursa-pastoris* have been applied in offshore or land-based Multi-Trophic Aquaculture (IMTA) systems (Lothmann and Sewilam, 2023). Moreover, *Kappaphycus alvarezii* (Hayashi et al., 2008), *Gracilariopsis longissima* (He et al., 2014), *Caulerpa lentillifera* (Bambaranda et al., 2019), kelps (e.g., *Nereocystis luetkeana*; (Supratya and Martone, 2024), *Sargassum siliquosum* (Edwards et al., 2024) have received increasing attention. In recent years, *Ulva prolifera* (*U. prolifera*) has garnered significant research interest due to its exceptional capacity for nitrogen and phosphorus assimilation, combined with its frequent bloom events (Xia et al., 2024). Since 2008, recurrent green tide events in the Southern Yellow Sea of China have necessitated substantial resource allocation for shoreline cleanup of macroalgal deposits (Sun et al., 2022). The accumulation of drifting algae along coastlines (driven by ocean currents and tidal dynamics) has disrupted local aquaculture operations, resulting in significant economic losses (Liu et al., 2022). As the dominant species in green tide events, *U. prolifera* demonstrates significantly superior nitrogen and phosphorus absorption, enrichment, and assimilation capabilities compared to other macroalgae (Wu et al., 2025a). This proven physiological capacity qualifies it as a promising biofilter material for treating aquaculture wastewater, particularly in RAS. However, the research on the effects of different initial concentrations of nitrogen and different forms of nitrogen on the absorption rate of *U. prolifera* is still insufficient. This study aims to (1) analyze the adsorption kinetics and nitrogen source preference (NH_4^+, NO_2^- and NO_3^-) of *U. prolifera* at varying initial concentrations, (2) quantify its nitrogen removal capacity from aquaculture effluents, and (3) provide foundational data to advance IMTA systems.

2 Materials and methods

2.1 Material sources and pretreatment

The green algae (*U. prolifera*) was obtained from the Algal Laboratory of the Water Environment & Ecology Engineering Research Center of Shanghai Institution of Higher Education at Shanghai Ocean University. It was collected during the green tide outbreak in 2021 from the coastal waters near Qingdao, Shandong Province (36°3′48″N, 120°23′34″E), preserved in ice boxes, and transported to the laboratory within 48 hours for processing. After isolation and purification, the strain was preserved in the

laboratory. Subsequently, molecular identification was conducted on the algae. Internal transcribed spacer (ITS) sequences and 5S ribosomal deoxyribonucleic acid (5S rDNA) spacer sequences were chosen for species identification, and the algal species was identified as *Ulva prolifera* (sequencing data can be found in the Supplementary Materials).

For large-scale cultivation, *U. prolifera* was pre-cultured in 1 L custom-made round glass containers. The culture medium consisted of artificial seawater prepared using sea salt crystals (Lanhongxing brand, Haiding Technology, Shanghai), which was filtered, sterilized, and supplemented with VSE nutrients, with a salinity of 24 ± 0.2 psu. Cultivation conditions were as follows: temperature 22 ± 1°C, light intensity 90 μmol·m^{-2}·s^{-1}, 12-hour light:12-hour dark photoperiod, and continuous aeration. These parameters ensured optimal growth conditions for *U. prolifera* (Huo et al., 2021; Bao et al., 2023; Glauco et al., 2024). The algae were cultured for 30 days prior to the experiment to ensure availability for experimental use.

2.2 Experimental design

The inorganic nitrogen content in seawater of routinely cultured *U. prolifera* was measured daily until it reached zero (below the detection limit). No additional nitrogen nutrients were supplemented thereafter, and the algae were maintained under nitrogen starvation for 7 days before nitrogen uptake kinetics experiments.

Using artificial seawater without additional nitrogen sources as the baseline (NH_4^+-N: 0.25 μmol·L^{-1}, NO_3^--N: 4.9 μmol·L^{-1}, NO_2^--N: 0.07 μmol·L^{-1}, PO_4^{3-}-P: 0.02 μmol·L^{-1}), seawater with varying initial nitrogen concentrations was prepared by adding high-concentration NH_4Cl, $NaNO_3$, and $NaNO_2$ solutions. Both the artificial seawater and all nitrogen stock solutions (NH_4Cl, $NaNO_3$, and $NaNO_2$ prepared to target concentrations) were autoclaved to prevent microbial interference with nitrogen transformation processes. Three nitrogen species were tested at eight gradient concentrations:

NH_4^+-N: 0.5, 5, 10, 15, 20, 25, 30, 35 μmol·L^{-1};

NO_3^--N: 5, 10, 20, 30, 60, 90, 110, 130 μmol·L^{-1};

NO_2^--N: 2.5, 5, 10, 15, 20, 30, 50, 60 μmol·L^{-1}.

Each concentration had three replicates, totaling 72 samples. Each sample contained 1 L of seawater and 2.0 ± 0.05 g of nitrogen-starved *U. prolifera*, with other cultivation conditions consistent with prior protocols.

Water samples (5 mL) were collected at 0 h, 1 h, 2 h, 4 h, and 6 h after the experiment initiation. The removed volume was immediately replenished with artificial seawater to maintain a constant total volume. The concentrations of different nitrogen species in the seawater were measured at each time point. After the experiment, the *U. prolifera* was collected, dried at 60 °C to constant weight, and its dry weight was determined.

2.3 Data and statistical analysis

The formulas for calculating the absorption rate (V), maximum absorption rate (V_{max}), and Michaelis constant (K_m) of *U. prolifera* for inorganic nitrogen components are as follows:

$$V = \frac{(C_{t-1} - C_t) \cdot V_{t-1}}{t \cdot W} \quad (1)$$

Where V means absorption rate (μmol·g^{-1}·h^{-1}), C_{t-1} and C_t means initial and final nutrient concentrations (μmol·L^{-1}) during the sampling interval, V_{t-1} means initial culture volume (L) during the interval, t means time interval (h), and W means dry weight of algae (g).

Michaelis-Menten kinetics equation is as follows:

$$V = \frac{V_{\max} \times C}{K_m + C} \quad (2)$$

Where V means absorption rate (μmol·g^{-1}·h^{-1}), V_{max} means maximum absorption rate (μmol·g^{-1}·h^{-1}), K_m means Michaelis constant (μmol·L^{-1}), C means initial nutrient concentration (μmol·L^{-1}) during the sampling interval.

Experimental data were preprocessed using Excel, analyzed via one-way ANOVA and variance tests in SPSS 26.0 with a significance level of $P < 0.05$, and visualized using Origin 2022.

3 Results

3.1 The influence of different initial concentrations on the adsorption of NO_2^--N by *U. prolifera*

Changes in NO_2^--N concentration within the culture media across treatment groups are shown in Figure 1. *U. prolifera* exhibited significant absorption of NO_2^--N. In low-concentration groups (2.5 and 5 μmol·L^{-1}), NO_2^--N was completely depleted within 2 h. In contrast, high-concentration groups (30, 50, 60 μmol·L^{-1}) showed a gradual decline in NO_2^--N concentration over time. After 6 h, the cumulative NO_2^--N removal capacity ranked as follows: 50 > 30 > 60 > 20 > 15 > 10 > 5 > 2.5 μmol·L^{-1} groups. The highest total removal occurred in the 50 μmol/L group (38.72 μmol), followed by the 30 μmol/L group (30.31 μmol).

The NO_2^--N absorption rate per unit algal biomass (Calculated by Equation 1; μmol·g^{-1}·h^{-1}) is presented in Figure 2. In 0–1 h, all groups reached peak absorption rates, indicating rapid initial uptake by nitrogen-starved *U. prolifera*. Absorption rates increased with initial concentration but were suppressed at concentrations >50 μmol·L^{-1} (Figure 2a). In 1–2 h, high-concentration groups (60 μmol·L^{-1}) continued to inhibit absorption rates (Figure 2b). Notably, during the initial absorption phase (1–2 h), the NO_2^--N uptake rates demonstrated sufficient normality across concentration gradients (2.5-60

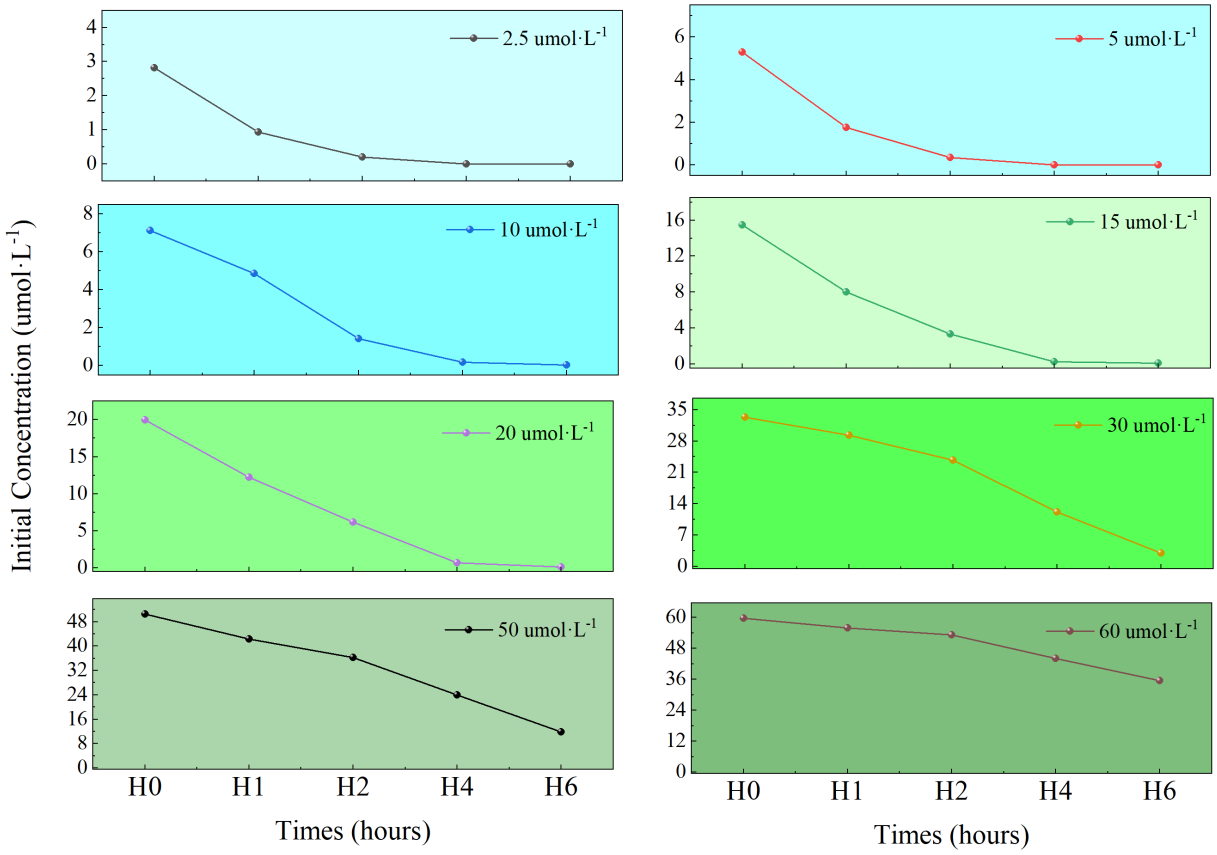

FIGURE 1
The variation of NO_2^--N concentration under different initial concentrations in medium.

μmol·L^{-1}), validating their applicability for kinetic modeling via the Michaelis-Menten equation (Figure 2b). In 2–6 h, absorption rates dropped to 0 μmol·g^{-1}·h^{-1} in low-concentration groups (2.5-20 μmol·L^{-1}) due to substrate depletion (Figures 2c, d). After 6 h, NO_2^--N removal efficiencies (%) for each initial concentration group (2.5-60 μmol·L^{-1}) were: 99%, 100%, 99%, 99%, 99%, 91%, 77%, and 41%. These results demonstrate that NO_2^--N concentrations exceeding 50 μmol·L^{-1} significantly suppress the absorption capacity of *U. prolifera*.

3.2 The influence of different initial concentrations on the adsorption of NO_3^--N by *U. prolifera*

Changes in NO_3^--N concentration within the culture media across treatment groups are shown in Figure 3. *U. prolifera* exhibited significant absorption capacity for nitrate nitrogen (NO_3^--N). In low-concentration groups (5-30 μmol·L^{-1}), NO_3^--N was almost completely depleted within 1–2 h. High-concentration groups (110-130 μmol·L^{-1}) showed gradual declines in NO_3^--N concentration over time. After 6 h, the cumulative NO_3^--N removal ranked as: 130 > 110 > 90 > 60 > 30 > 20 > 10 > 5 μmol·L^{-1} groups, with the highest total removal in the 130 μmol·L^{-1} group (100.25 μmol) followed by the 110 μmol/L group (96.15 μmol).

Time-dependent absorption rates (μmol·g^{-1}·h^{-1}) are shown in Figure 4. In 0–1 h, all groups except 130 μmol·L^{-1} reached peak absorption rates, and absorption suppression occurred in high-concentration groups (≥110 μμmol·L^{-1}) (Figure 4a). In 2–4 and 4–6 h, rates dropped to 0 μmol·g^{-1}·h^{-1} in low-concentration groups (5-30 μmol·L^{-1}) due to substrate exhaustion (Figures 4c, d). Final NO_3^--N removal efficiencies (%) per group (5-130 μmol·L^{-1}) were: 31%, 100%,100%, 100%, 100%, 100%, 87% and 77%. It is worth noting that the NO_3^--N removal rate in the lowest concentration group (5 μmol·L^{-1}) did not reach 100%, which indicates that in addition to the high concentration inhibition of NO_3^--N absorption by *U. prolifera*, there may also be a low concentration absorption threshold.

3.3 The influence of different initial concentrations on the adsorption of NH_4^+-N by *U. prolifera*

Changes in NH_4^+-N concentration within the culture media across treatment groups are shown in Figure 5. *U. prolifera* demonstrated significant assimilation capacity for ammonium nitrogen (NH_4^+-N). In low concentration groups (0.5-15 μmol·L^{-1}), NH_4^+-N was fully depleted within 2 h. High-concentration groups (20-35 μmol·L^{-1}) exhibited gradual concentration declines throughout the experiment. After 6 h, cumulative NH_4^+-N removal

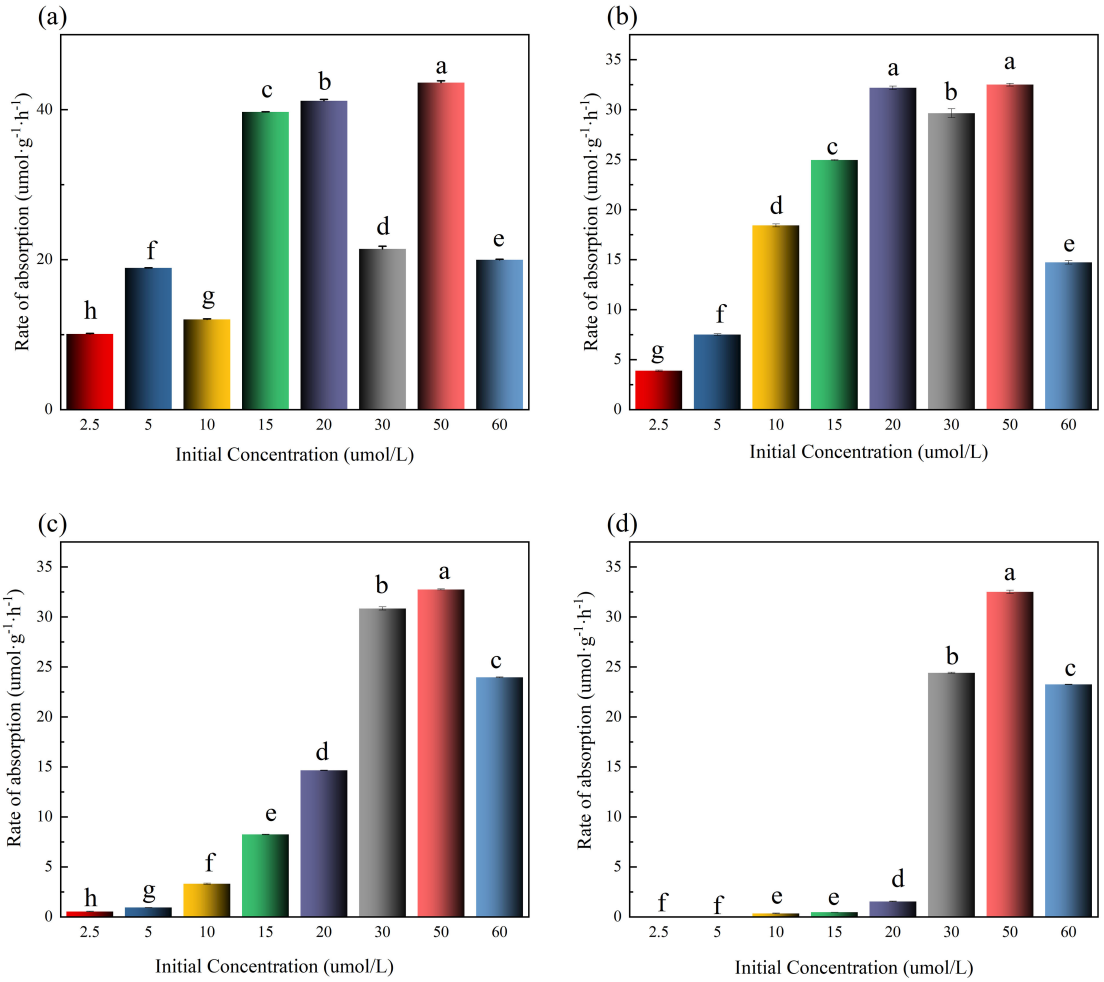

FIGURE 2
Rate of absorption in different initial concentrations of NO_2^--N in medium (The lowercase letters denote statistically significant differences between groups at $P < 0.05$ based on Tukey's honestly significant difference (HSD) post hoc test. Groups sharing the same letter indicate no significant difference).

ranked per group (0.5-35 μmol·L^{-1}) as: 30 > 20 > 25 > 35 > 15 > 10 > 5 > 0.5 μmol·L^{-1} groups, with maximum removal in the 30 μmol·L^{-1} group (18.08 μmol) followed by the 20 μmol/L group (17.04 μmol).

Figure 6 illustrates time-dependent NH_4^+-N absorption kinetics in *U. prolifera*. In 0–1 h, all treatment groups exhibited peak absorption rates (Figure 6a), indicating rapid initial uptake of NH_4^+-N by nitrogen-starved algae. In 1–2 h, high concentrations (≥15 μmol·L^{-1}) suppressed absorption rates (Figure 6b). In 2–4 and 4–6 h, absorption dropped to 0 μmol·g^{-1}·h^{-1} in low-concentration groups (0.5-15 μmol·L^{-1}) due to substrate depletion (Figures 6c, d). After 6 h, NH_4^+-N removal efficiencies were: 100%, 100%, 100%, 100%, 100%, 79%, 88% and 64%.

3.4 The absorption kinetics characteristics of *U. prolifera* under different nitrogen forms

The 1–2 h interval was selected for Michaelis-Menten modeling (Calculated by Equation 2 due to its strong linear correlation and homogeneous data distribution across nitrogen species. Fitted kinetic parameters for NO_2^-–N, NO_3^-–N, and NH_4^+–N assimilation are summarized in Table 1.

Kinetic analysis revealed distinct nitrogen assimilation patterns in *U. prolifera*: The maximum uptake velocity (V_{max}) followed NO_3^-–N (161.29 μmol·g^{-1}·h^{-1}) > NO_2^-–N (39.06 μmol·g^{-1}·h^{-1}) > NH_4^+–N (27.17 μmol·g^{-1}·h^{-1}), demonstrating superior nitrate removal capacity, while half-saturation constants (K_m) exhibited NH_4^+–N (4.60 μmol·L^{-1})< NO_2^-–N (8.31 μmol·L^{-1})< NO_3^-–N (29.40 μmol·L^{-1}), indicating highest transporter affinity for ammonium. This inverse relationship between V_{max} and K_m values elucidates a competitive assimilation priority: the minimal K_m for NH_4^+–N drives preferential uptake during multi-nitrogen co-exposure, aligning with energy conservation strategies in algal metabolism where ammonium assimilation consumes less energy than nitrate assimilation.

NH_4^+–N can be directly absorbed by algae and incorporated into amino acids such as glutamine, a process catalyzed by glutamine synthetase (GS) and glutamate synthase (GOGAT) (Guo et al., 2024). Because NH_4^+–N is already in a reduced state, algae do not

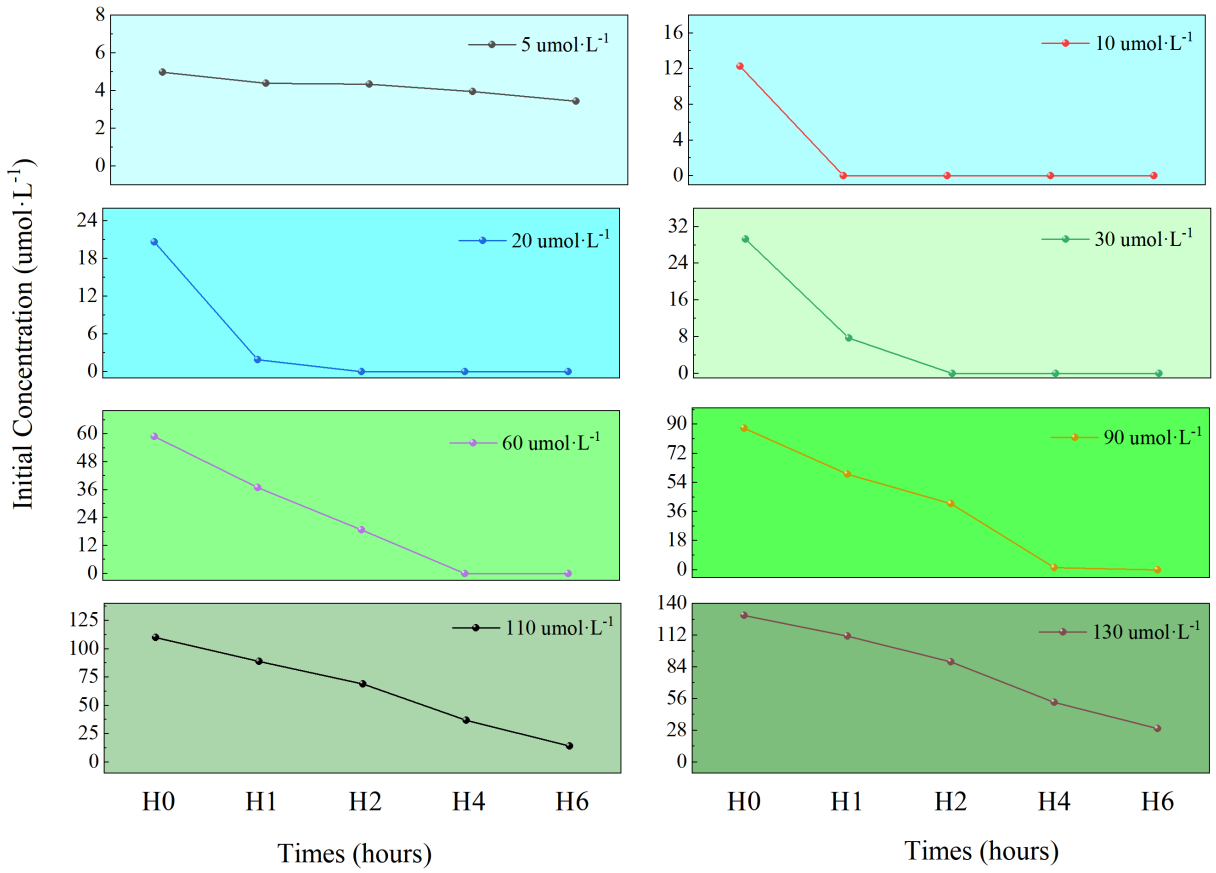

FIGURE 3
The variation of NO_3^--N concentration under different initial concentrations in medium.

need additional energy for reduction, making NH_4^+-N assimilation the most energetically economical (Pereira and Cushman, 2019). NO_3^-–N must first be reduced to nitrite by nitrate reductase (NR) and then to NH_4^+–N by nitrite reductase (NiR) (Xu et al., 2024). Both reduction steps require energy input, usually provided in the form of NAD(P)H or reduced ferredoxin. Therefore, NO_3^-–N assimilation requires more energy than NH_4^+–N assimilation. NO_2^-–N is an intermediate product in the reduction of NO_3^-–N to NH_4^+–N. Therefore, algae absorbing NO_2^-–N only require one reduction step (converting to NH_4^+–N via NO_2^-–N reductase), making it more efficient than NO_3^-–N assimilation but still requiring more energy than directly absorbing NH_4^+–N (Córdoba et al., 1986). Energy conservation strategies explain the differences among the three K_m to some extent. The energy conservation strategy partially explains the differences in K_m among the uptake of the three nitrogen forms.

3.5 The optimal applicable conditions for *U. prolifera* to absorb different forms of nitrogen

U. prolifera cannot sustain rapid nitrogen assimilation indefinitely as a biofilter, justifying our kinetic modeling focus on the 1–2 h window where initial surge uptake reflects nitrogen starvation pretreatment while phase-II steady-state absorption aligns with practical operations. Nitrogen assimilation dynamics—modulated by temperature, pH, irradiance, salinity, phosphorus limitation, and initial N concentration—were evaluated under optimized conditions (24°C, 90 μmol photons·m^{-2}·s^{-1}, salinity 22 PSU), revealing two critical operational thresholds including non-inhibitory optimal concentrations (50 μmol·L^{-1} NO_2^--N, 90 μmol·L^{-1} NO_3^--N, 20 μmol·L^{-1} NH_4^+-N) and V_{max}-sustaining concentrations derived from K_m values (NO_2^--N =8.3 μmol·L^{-1}, NO_3^--N =29.4 μmol·L^{-1}, NH_4^+-N =4.6 μmol·L^{-1}). For recirculating aquaculture systems experiencing dynamic nitrogen fluctuations, adaptive biomass deployment becomes essential requiring a 1.5-2× increase in *U. prolifera* biomass when total inorganic nitrogen exceeds 20 mg/L to sustain >90% removal efficiency.

4 Discussion

4.1 The absorption kinetics characteristics *of U. prolifera* for different nitrogen forms

This study provides the systematic characterization of NH_4^+-N, NO_3^--N, and NO_2^--N uptake kinetics in *U. prolifera* using

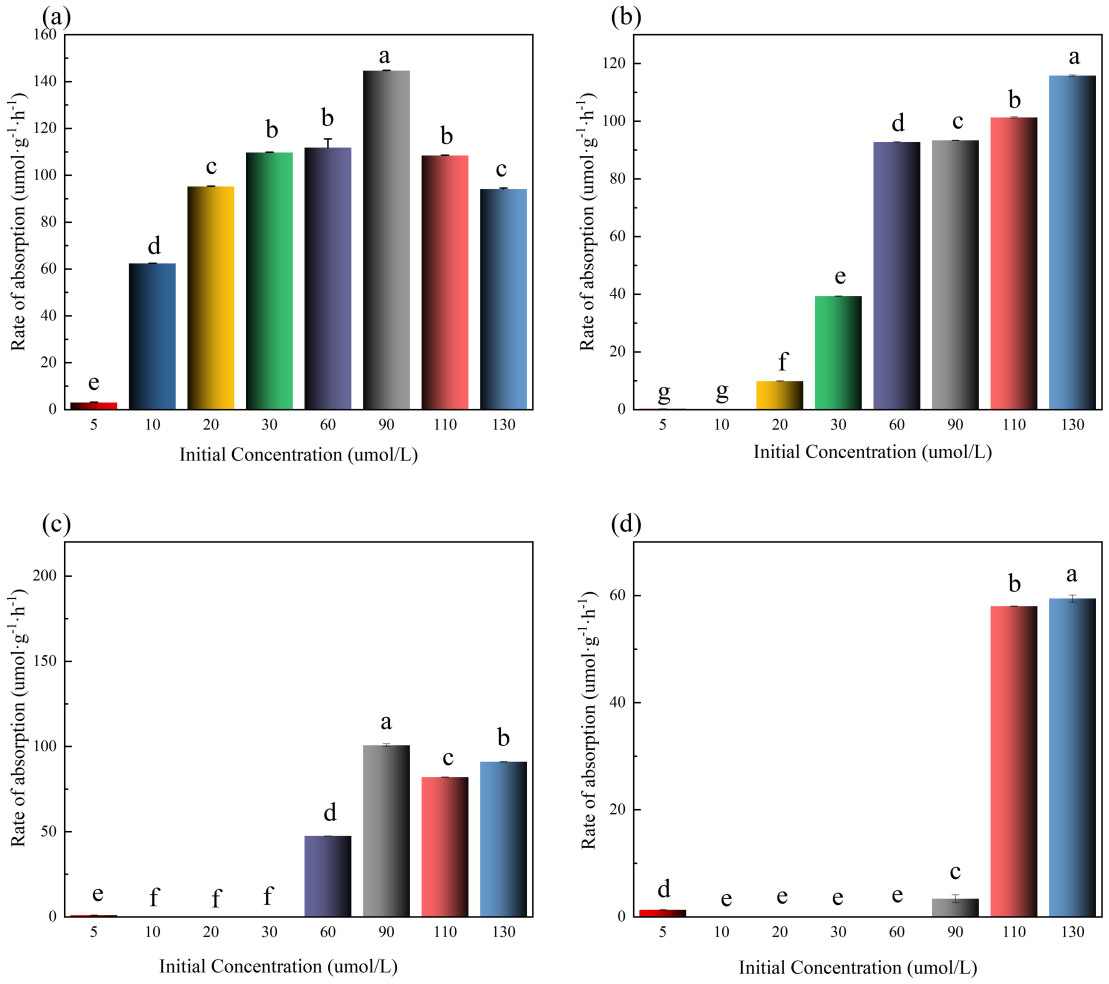

FIGURE 4
Rate of absorption in different initial concentrations of NO_3^--N in medium. The lowercase letters denote statistically significant differences between groups at $P < 0.05$ based on Tukey's honestly significant difference (HSD) post hoc test. Groups sharing the same letter indicate no significant difference.

Michaelis-Menten modeling. The relationship between the N absorption rate of large seaweeds and the concentration of nutrients generally follows the deformation formula of the Michaelis-Menten equation: $V=V_{max} \cdot C/(K_m+C)$. *U. prolifera* as a species of large seaweed, also follows this rule (Luo et al., 2012; Zhang et al., 2019). The differential kinetic parameters reveal profound physiological adaptations of *U. prolifera* to environmental nitrogen regimes. *U. prolifera* exhibits robust uptake capacity for all three inorganic nitrogen forms. Notably, its maximum NO_3^--N absorption velocity reaches 161.29 $\mu mol \cdot g^{-1} \cdot h^{-1}$. This high NO_3^--N assimilation efficiency aligns with nitrate's dominance in natural marine environments, likely reflecting long-term evolutionary adaptation between coastal macroalgae and NO_3^--N dominated seawater.

NH_4^+-N exhibited the highest substrate affinity (K_m = 4.60 $\mu mol \cdot L^{-1}$, R^2 = 0.99). This preference likely stems from the lower energy cost of NH_4^+–N assimilation compared to other nitrogen sources, as NO_2^--N or NO_3^--N are more oxidized forms of nitrogen that need to be reduced to NH_4^+-N (Abreu et al., 2011; Li et al., 2016; Ross et al., 2018). NH_4^+-N is commonly taken up through passive diffusion. As nitrogen is presented in a reduced state that can be easily assimilated, the uptake rate rises in proportion to the substrate concentration. In contrast, NO_3^--N must first undergo reduction to NO_2^--N and then to NH_4^+-N before algae can utilize this nitrogen source. This makes nitrogen uptake an energy dependent process (Fan et al., 2014). In practice, high substrate affinity enables sustained high absorption efficiency (100% removal within 6 h) at ammonium concentrations ≤20 $\mu mol \cdot L^{-1}$. Notably, field measurements confirm that NH_4^+-N levels in both the green tide origin site (Subei Shoal: about 10.79 $\mu mol \cdot L^{-1}$) and landing area (Qingdao coast: about 2.87 $\mu mol \cdot L^{-1}$) remain consistently<20 $\mu mol \cdot L^{-1}$ (Wu et al., 2025b; Xiu et al., 2019). Consequently, *U. prolifera* experiences no NH_4^+-N inhibition during floating dispersal, as ambient concentrations remain below the suppression threshold identified in kinetic assays. This might also be one of the reasons for the rapid growth of *U. prolifera* biomass during the outbreak of the green tide.

NO_3^--N dominates the dissolved nitrogen pool in seawater, and the high uptake capacity of *U. prolifera* for NO_3^--N (V_{max}= 161.29 $\mu mol \cdot g^{-1} \cdot h^{-1}$, *R2* = 0.99) represents a significant ecological

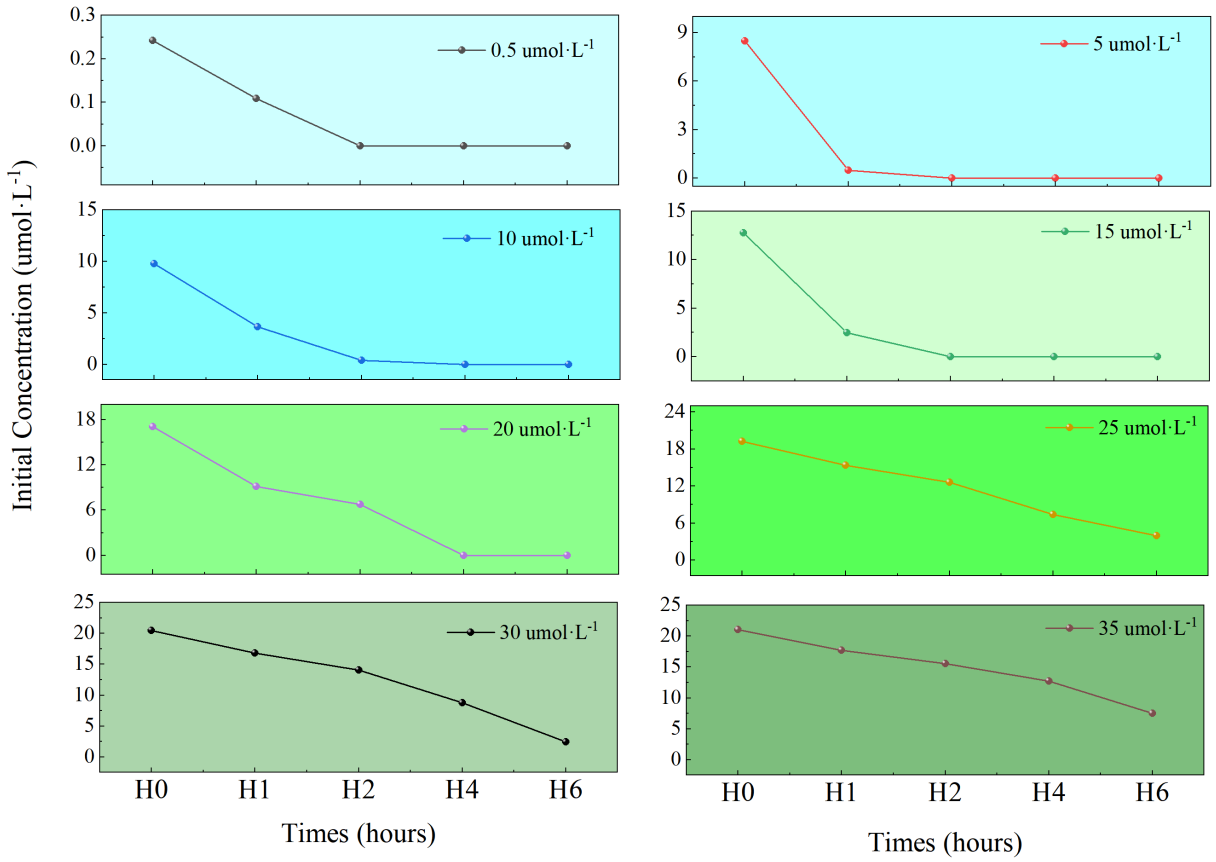

FIGURE 5
The variation of NH_4^+-N concentration under different initial concentrations in medium.

adaptation. This confers competitive advantage in nutrient acquisition within complex nitrogen matrices. Evidence suggests NO_3^- may be the preferred nitrogen form for *U. prolifera* growth (Li et al., 2019), with uptake rates increasing proportionally to ambient nitrate concentrations (Zhang et al., 2021). According to the dual-compartment model established by Heimer and Filner (Heimer and Filner, 1971), nitrate is stored primarily in vacuoles (occupying ≈90% of cell volume), while metabolic nitrate resides in the cytoplasm. This explains the high absorption and enrichment capacity of NO_3^--N by *U. prolifera*. In addition, *U. prolifera* still maintained a removal rate of 77% - 87% at a concentration of 90-110 μmol·L^{-1} (Figure 4), confirming its potential as a RAS biological filter.

NO_2^--N uptake kinetics exhibited a distinct unimodal curve: removal efficiency exceeded ≥99% at ≤20 μmol·L^{-1} but plummeted to 41% at >50 μmol·L^{-1} within 6 h (Figure 2). Although its K_m (8.31 μmol·L^{-1}) was lower than that of NO_3^--N, the inhibition under elevated concentrations was more pronounced. For a long time, NO_2^--N has been ignored, although it is toxic to aquatic organisms. Interestingly, *U. prolifera* has a strong absorption capacity for NO_2^--N, which will effectively alleviate the toxicity caused by the accumulation of NO_2^--N in RAS.

The process of nitrogen within the cell mainly involves NO_3^--N accumulating in the vacuole and cytoplasm. NO_3^--N is reduced to NO_2^--N through nitrate reductase (NR). Then, NO_2^--N diffuses onto the cell membrane in a molecular form. Subsequently, under the action of nitrite reductase (NiR), it is converted into NH_4^+-N, serving as the substrate for amino acid synthesis (Zhang et al., 2021). Therefore, when the concentration of NO_2^--N is too high, the nitrite reduction process in the cell is inhibited, and the absorption of NO_2^--N by algae slows down. In summary, the kinetic characteristics of "low NH_4^+-N affinity - high NO_3^--N capacity - NO_2^--N sensitivity" of *Ulva* are the core of its green tide competitive advantage and provide a basis for nitrogen form regulation in RAS. That is, prioritizing the control of NH_4^+-N can alleviate the nitrification load, but the toxic threshold of NO_2^--N needs to be avoided.

4.2 The influence of initial concentration and time on absorption kinetics

Initial concentration gradient experiments have exposed *Ulva*'s nonlinear nitrogen uptake response. NH_4^+-N uptake was

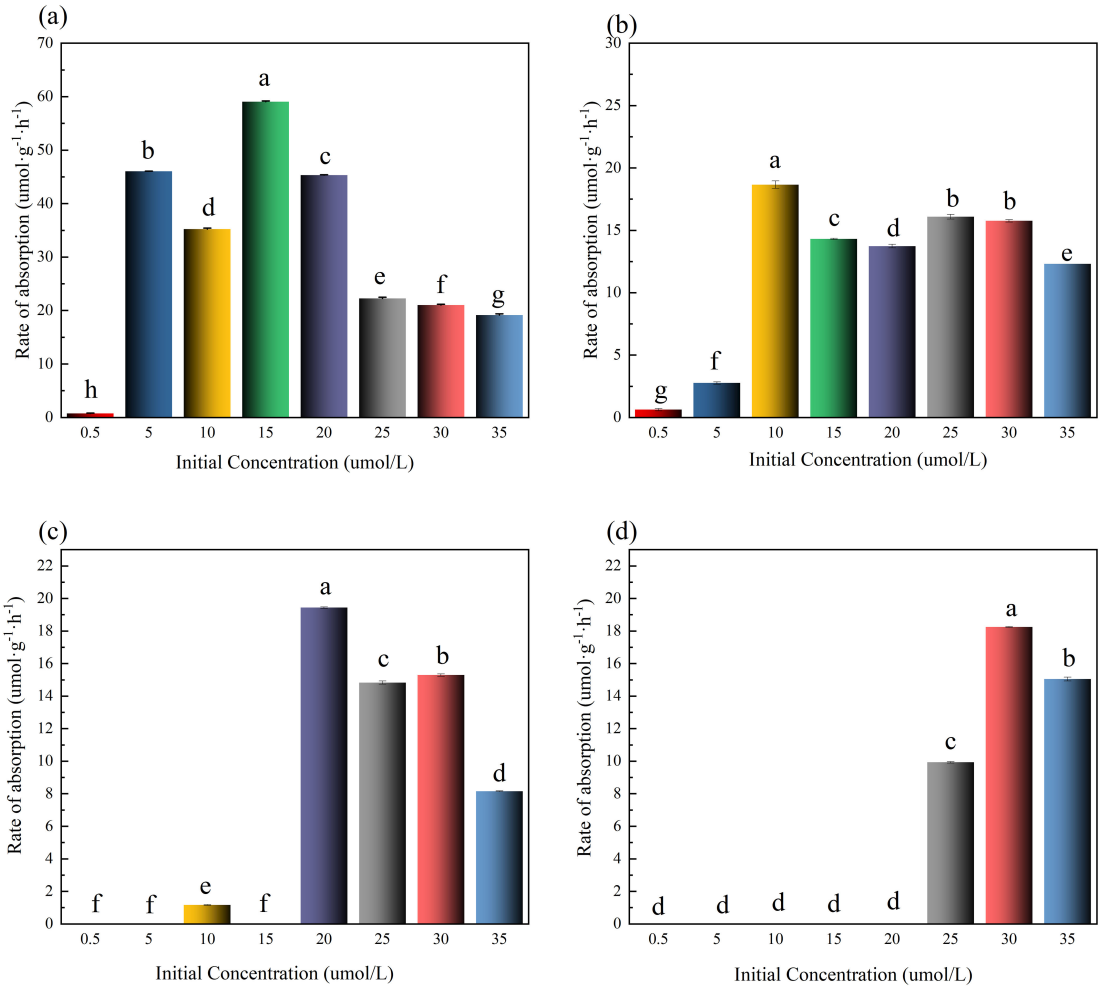

FIGURE 6
Rate of absorption in different initial concentrations of NH_4^+-N in medium. The lowercase letters denote statistically significant differences between groups at $P < 0.05$ based on Tukey's honestly significant difference (HSD) post hoc test. Groups sharing the same letter indicate no significant difference.

TABLE 1 Estimated kinetic parameters for NO2–N, NO3–N, NH4+-N uptaking.

Inorganic nitrogen form	Interval (h)	V_{max} (μmol·g^{-1}·h^{-1})	K_m (μmol·L^{-1})	R^2
$NO2^-$–N	1-2h	39.06	8.31	0.95
$NO3^-$–N	1-2h	161.29	29.40	0.99
NH_4^+-N	1-2h	27.17	4.60	0.99

proportional to concentration from 0.5 to 20 μmol·L^{-1}, but the removal rate dropped 40%–60% when levels exceeded 20 μmol·L^{-1}. NO_3^--N uptake kept high absorption rate from 5 to 90 μmol·L^{-1}, yet was restrained once concentrations surpassed 110 μmol·L^{-1}. For NO_2^--N, remarkable inhibition occurred above 30 μmol·L^{-1}, with the 60 μmol·L^{-1} group achieving merely a 41% removal rate after 6 hours. This reflects *Ulva*'s varied response to different nitrogen concentrations and confirms the high ecological risk of elevated NO_2^--N levels.

The absorption process displayed a three phase evolution. During the rapid absorption phase (0–1 hour), nitrogen - starved transporters reacted swiftly, enabling all groups to reach peak absorption rates. In the steady - state phase (1–2 hours), absorption neared V_{max}, aligning with the Michaelis - Menten model, which made it the ideal window for kinetic modeling. During the attenuation phase (2–6 hours), low concentration groups (NO_3^--N ≤15, NO_3^--N ≤30, NO_2^--N ≤20 μmol·L^{-1}) plateaued due to substrate depletion, while high concentration groups were governed by inhibitory effects.

TABLE 2 Reference for the removal rate during the actual operation of RAS.

Biomass	Nitrogen form	Time interval	Velocity at different initial concentrations							
			2.5	5	10	15	20	30	50	60
1g	NO_2^-	0-1	10.08	18.87	12.02	39.69	41.17	21.42	43.61	19.98
		1-2	3.88	7.50	18.42	24.96	32.19	29.64	32.49	14.73
		2-4	0.53	0.93	3.31	8.24	14.65	30.84	32.74	23.95
		4-6	0.00	0.00	0.34	0.46	1.54	24.41	32.51	23.25
Final removal rate			99%	100%	99%	99%	99%	91%	77%	41%
1g	NO_3^-		5	10	20	30	60	90	110	130
		0-1	2.99	62.38	95.21	109.71	111.76	144.61	108.43	94.10
		1-2	0.26	0.00	9.83	39.35	92.74	93.33	101.27	115.77
		2-4	0.98	0.00	0.00	0.00	47.44	100.71	81.99	90.95
		4-6	1.32	0.00	0.00	0.00	0.00	3.38	58.01	59.42
Final removal rate			31%	100%	100%	100%	100%	100%	87%	77%
1g	NH_4^+		0.5	5	10	15	20	25	30	35
		0-1	0.77	46.02	35.24	59.04	45.30	22.27	21.01	19.15
		1-2	0.62	2.76	18.66	14.30	13.73	16.09	15.76	12.31
		2-4	0.00	0.00	1.16	0.00	19.43	14.83	15.29	8.15
		4-6	0.00	0.00	0.00	0.00	0.00	9.93	18.25	15.05
Final removal rate			100%	100%	100%	100%	100%	79%	88%	64%

we consider the initial concentration at which a high removal efficiency is maintained (over 90% for 6 hours) as the upper limit of the concentration of the tail water from algae filtration. As show in Table 2, based on these findings, the following RAS application strategy is proposed: limiting NH_4^+-N to ≤20 μmol·L^{-1}, NO_3^--N to ≤90 μmol·L^{-1}, and NO_2^--N to ≤30 μmol·L^{-1} to prevent inhibition; boosting *Ulva* biomass by 1.5–2 times when TIN is high; and using pulsed feeding or continuous - flow reactors to avoid efficiency loss from algal nitrogen saturation.

4.3 Limitations and future perspectives

The limitations of this study are as follows: PO_4^{3-} -P was fixed at 0.02 μmol·L^{-1} (Real seawater levels), so the impact of N:P ratio fluctuations on kinetics wasn't investigated; urea and other organic nitrogen, which account for 15% – 30% of aquaculture wastewater, weren't covered; and the single nitrogen source experiments failed to reflect the real environment with multiple coexisting nitrogen sources.

Future research should focus on the following aspects: integrating RAS nitrogen emission temporal data to build dynamic models; leveraging the high V_{max} characteristics of green - tide strains (e.g., NO_3^--N V_{max} = 161.29 μmol·g^{-1}·h^{-1}) and CRISPR technology to enhance nitrogen transporter genes; developing a "negative - emission" RAS system that integrates *Ulva* carbon fixation with nitrogen removal; and using transcriptomics to analyze NO_2^--N inhibition mechanisms for designing resistant algal strains.

5 Conclusion

The nitrogen uptake kinetics of *U. prolifera* constitute a fundamental mechanism underpinning both its ecological competitive advantage and bioremediation potential. This study quantified species-specific nitrogen uptake kinetics, revealing a physiological strategy characterized by: (i) optimal substrate affinity for NH_4^+-N (K_m = 4.60 μmol·L^{-1}), (ii) high uptake capacity for NO_3^--N (V_{max} = 161.29 μmol·g^{-1}·h^{-1}), and (iii) sensitive yet efficient NO_2^--N absorption (V_{max} = 39.06 μmol·g^{-1}·h^{-1}). Optimizing concentration thresholds and biomass allocation enables synergistic aquaculture wastewater denitrification and biomass valorization. Future research should prioritize elucidating multi-nitrogen interaction mechanisms and integrated process engineering. This dual functionality positions *U. prolifera* as a nature based solution for sustainable aquaculture, specifically contributing to SDG 6 (Clean Water) and SDG 14 (Life Below Water) through nitrogen bioremediation and biomass valorization in RAS.

Data availability statement

The original contributions presented in the study are included in the article/Supplementary Material. Further inquiries can be directed to the corresponding authors or the first author.

Author contributions

WL: Investigation, Conceptualization, Resources, Writing – original draft. MZ: Investigation, Writing – original draft, Resources, Conceptualization. XX: Validation, Writing – original draft, Methodology. CH: Supervision, Funding acquisition, Writing – review & editing, Project administration. JL: Project administration, Writing – review & editing, Supervision, Funding acquisition. PH: Supervision, Writing – original draft, Writing – review & editing, Project administration, Funding acquisition.

Funding

The author(s) declare financial support was received for the research and/or publication of this article. This work was supported by the National Key Research & Development Program of China (Grant No. 2024YFC3109000).

Acknowledgments

All the authors express their gratitude to the reviewers and editors for their support and efforts in improving the quality of the manuscript. In particular, we are grateful to the journal manager Joanna Johnson for the assistance provided in reducing our APC.

Conflict of interest

The authors declare that the research was conducted in the absence of any commercial or financial relationships that could be construed as a potential conflict of interest.

Generative AI statement

The author(s) declare that Generative AI was used in the creation of this manuscript. AI is used for language polishing.

Publisher's note

Supplementary material

The Supplementary Material for this article can be found online at: https://www.frontiersin.org/articles/10.3389/fmars.2025.1654677/full#supplementary-material

References

Abreu, M. H., Pereira, R., Buschmann, A. H., Sousa-Pinto, I., and Yarish, C. (2011). Nitrogen uptake responses of *Gracilaria vermiculophylla* (Ohmi) Papenfuss under combined and single addition of nitrate and ammonium. *J. Exp. Mar. Biol. Ecol.* 407, 190–199. doi: 10.1016/j.jembe.2011.06.034

Ahmed, N., Thompson, S., and Glaser, M. (2019). Global aquaculture productivity, environmental sustainability, and climate change adaptability. *Environ. Manage* 63, 159–172. doi: 10.1007/s00267-018-1117-3

Ahmed, N., and Turchini, G. M. (2021). Recirculating aquaculture systems (RAS): Environmental solution and climate change adaptation. *J. Clean Prod* 297, 126604. doi: 10.1016/j.jclepro.2021.126604

Bambaranda, B. M., Tsusaka, T. W., Chirapart, A., Salin, K. R., and Sasaki, N. (2019). Capacity of *Caulerpa lentillifera* in the removal of fish culture effluent in a recirculating aquaculture system. *Processes* 7, 440. doi: 10.3390/pr7070440

Bao, M., Xing, Q., Park, J. S., He, P., Zhang, J., Yarish, C., et al. (2023). Temperature and high nutrients enhance hypo-salinity tolerance of the bloom forming green alga, *Ulva prolifera*. *Harmful Algae* 123, 102402. doi: 10.1016/j.hal.2023.102402

Cahill, P. L., Hurd, C. L., and Lokman, M. (2010). Keeping the water clean - Seaweed biofiltration outperforms traditional bacterial biofilms in recirculating aquaculture. *Aquaculture* 306, 153–159. doi: 10.1016/j.aquaculture.2010.05.032

Córdoba, F., Cárdenas, J., and Fernández, E. (1986). Kinetic characterization of nitrite uptake and reduction by chlamydomonas reinhardtii. *Plant Physiol.* 82, 904–908. doi: 10.1104/pp.82.4.904

Dalsgaard, J., Lund, I., Thorarinsdottir, R., Drengstig, A., Arvonen, K., and Pedersen, P. B. (2013). Farming different species in RAS in Nordic countries: Current status and future perspectives. *Aquacult Eng.* 53, 2–13. doi: 10.1016/j.aquaeng.2012.11.008

Edwards, G., Visch, W., Hurd, C. L., Smith, G., and Fitzgibbon, Q. (2024). Nitrogen excretion by the lobsters Panulirus ornatus and Thenus australiensis and uptake by the brown algae Sargassum siliquosum: Implications for integrated recirculated aquaculture systems. *Aquaculture* 581, 740486. doi: 10.1016/j.aquaculture.2023.740486

Fan, X., Xu, D., Wang, Y. T., Zhang, X. W., Cao, S. N., Mou, S. L., et al. (2014). The effect of nutrient concentrations, nutrient ratios and temperature on photosynthesis and nutrient uptake by *Ulva prolifera*: implications for the explosion in green tides. *J. Appl. Phycol* 26, 537–544. doi: 10.1007/s10811-013-0054-z

FAO (2019). Global aquaculture and capture production 1950–2017, Rome.

FAO (2024). World food and agriculture – statistical pocketbook, Rome.

Glauco, F., He, P., and Chen, Z. (2024). Combine effects of multiple environmental factors on growth and nutrient uptake of euryhaline seaweed growth in integrated multitrophic aquaculture systems. *Algal Res.* 77, 103347. doi: 10.1016/j.algal.2023.103347

Goddek, S., Delaide, B., Mankasingh, U., Ragnarsdottir, K. V., Jijakli, H., and Thorarinsdottir, R. (2015). Challenges of sustainable and commercial aquaponics. *Sustainability-Basel* 7, 4199–4224. doi: 10.3390/su7044199

Guo, H., Wang, W., Han, J., Zhu, J., Wang, Z., He, L., et al. (2024). Study on the characteristics and mechanism of inorganic nitrogen nutrients preferential assimilation by *Phaeocystis globosa*. *J. Mar. Sci. Eng.* 12, 989. doi: 10.3390/jmse12060989

Hayashi, L., Yokoya, N. S., Ostini, S., Pereira, R. T. L., Braga, E. S., and Oliveira, E. C. (2008). Nutrients removed by Kappaphycus alvarezii (Rhodophyta, Solieriaceae) in integrated cultivation with fishes in re-circulating water.. *Aquaculture* 277, 185–191. doi: 10.1016/j.aquaculture.2008.02.024

He, Q., Huo, Y., Zhang, J. H., Chai, Z. Y., Wu, H. L., Wen, S. S., et al. (2014). *Gracilariopsis longissima* as biofilter for an Integrated Multi-Trophic aquaculture (IMTA) system with: Bioremediation efficiency and production in a recirculating system. *Indian J. Geo-Mar Sci.* 43, 528–537.

Heimer, Y. M., and Filner, P. (1971). Regulation of the nitrate assimilation pathway in cultured tobacco cells. 3. The nitrate uptake system. *Biochim. Biophys. Acta* 230, 362–372. doi: 10.1016/0304-4165(71)90223-6

Huo, Y., Kim, J. K., Yarish, C., Augyte, S., and He, P. (2021). Responses of the germination and growth of *Ulva prolifera* parthenogametes, the causative species of green tides, to gradients of temperature and light. *Aquat. Bot.* 170, 103343. doi: 10.1016/j.aquabot.2020.103343

Kong, F. Z., Yu, R. C., Zhang, Q. C., Yan, T., and Zhou, M. J. (2012). Pigment characterization for the 2011 bloom in Qinhuangdao implicated "brown tide" events in China. *Chin. J. Oceanol Limn* 30, 361–370. doi: 10.1007/s00343-012-1239-z

Lavania-Baloo,, Azman, S., Said, M. I. M., Ahmad, F., and Mohamad, M. (2014). Biofiltration potential of macroalgae for ammonium removal in outdoor tank shrimp wastewater recirculation system. *Biomass Bioenerg* 66, 103–109. doi: 10.1016/j.biombioe.2014.02.031

Li, H., Cui, Z. G., Cui, H. W., Bai, Y., Yin, Z. D., and Qu, K. M. (2023). Hazardous substances and their removal in recirculating aquaculture systems: A review. *Aquaculture* 569, 739399. doi: 10.1016/j.aquaculture.2023.739399

Li, H. M., Zhang, Y. Y., Chen, J., Zheng, X., Liu, F., and Jiao, N. Z. (2019). Nitrogen uptake and assimilation preferences of the main green tide alga *Ulva prolifera* in the Yellow Sea, China. *J. Appl. Phycol* 31, 625–635. doi: 10.1007/s10811-018-1575-2

Li, H., Zhang, Y., Han, X., Shi, X., Rivkin, R. B., and Legendre, L. (2016). Growth responses of *Ulva prolifera* to inorganic and organic nutrients: Implications for macroalgal blooms in the southern Yellow Sea, China. *Sci. Rep-Uk* 6, 26498. doi: 10.1038/srep26498

Liu, J. L., Tong, Y. C., Xia, J., Sun, J. Y., Zhao, S., Zhuang, M. M., et al. (2022). Ulva macroalgae within local aquaculture ponds along the estuary of Dagu River, Jiaozhou Bay, Qingdao. *Mar. Pollut. Bull.* 174, 113243. doi: 10.1016/j.marpolbul.2021.113243

Lothmann, R., and Sewilam, H. (2023). Potential of innovative marine aquaculture techniques to close nutrient cycles. *Rev. Aquacult* 15, 947–964. doi: 10.1111/raq.12781

Luo, M. B., Liu, F., and Xu, Z. L. (2012). Growth and nutrient uptake capacity of two co-occurring species. *Aquat Bot.* 100, 18–24. doi: 10.1016/j.aquabot.2012.03.006

Mangott, A., Nappi, J., Carini, A. D., Goncalves, P., Hua, K., Domingos, J. A., et al. (2020). *Ulva lactuca* as a functional ingredient and water bioremediator positively influences the hepatopancreas and water microbiota in the rearing of Litopenaeus vannamei. *Algal Res.* 51, 102040. doi: 10.1016/j.algal.2020.102040

Nelson, S. G., Glenn, E. P., Conn, J., Moore, D., Walsh, T., and Akutagawa, M. (2001). Cultivation of Gracilaria parvispora (Rhodophyta) in shrimp-farm effluent ditches and floating cages in Hawaii: a two-phase polyculture system. *Aquaculture* 193, 239–248. doi: 10.1016/S0044-8486(00)00491-9

Pereira, P. N., and Cushman, J. C. (2019). Exploring the relationship between crassulacean acid metabolism (CAM) and mineral nutrition with a special focus on nitrogen. *Int. J. Mol. Sci.* 20, 4363. doi: 10.3390/ijms20184363

Randall, D. J., and Tsui, T. K. N. (2002). Ammonia toxicity in fish. *Mar. Pollut. Bull.* 45, 17–23. doi: 10.1016/S0025-326X(02)00227-8

Ross, M. E., Davis, K., McColl, R., Stanley, M. S., Day, J. G., and Semiao, A. J. C. (2018). Nitrogen uptake by the macro-algae *Cladophora coelothrix* and *Cladophora parriaudii*: Influence on growth, nitrogen preference and biochemical composition. *Algal Res.* 30, 1–10. doi: 10.1016/j.algal.2017.12.005

Shen, L., Wu, L., Wei, W., Yang, Y., MacLeod, M. J., Lin, J., et al. (2024). Marine aquaculture can deliver 40% lower carbon footprints than freshwater aquaculture based on feed, energy and biogeochemical cycles. *Nat. Food* 5, 615–624. doi: 10.1038/s43016-024-01004-y

Song, M. J., Yan, T., Kong, F. Z., Wang, Y. F., and Zhou, M. J. (2022). Increased diversity and environmental threat of harmful algal blooms in the Southern Yellow Sea, China. *J. Oceanol Limnol* 40, 2107–2119. doi: 10.1007/s00343-021-1209-4

Sun, Y. Q., Xia, Z. Y., Cao, X. L., Tong, Y. C., He, R. Y., Fu, M. L., et al. (2022). A mixed acid treatment for the prevention of *Ulva prolifera* attachment to *Neopyropia aquaculture* rafts: Laboratory experimentation. *Mar. Pollut. Bull.* 184, 114134. doi: 10.1016/j.marpolbul.2022.114134

Sun, Y. Q., Xia, Z. Y., Tong, Y. C., Li, S., Zhang, J. H., and He, P. M. (2024). Mixed acid treatment for removal of green macroalgae from *Neopyropia* aquaculture nets: Field experiment in the Subei Shoal, China. *Mar. Pollut. Bull.* 202, 116373. doi: 10.1016/j.marpolbul.2024.116373

Supratya, V. P., and Martone, P. T. (2024). Kelps on demand: Closed-system protocols for culturing large bull kelp sporophytes for research and restoration. *J. Phycol* 60, 73–82. doi: 10.1111/jpy.13413

Turcios, A. E., and Papenbrock, J. (2014). Sustainable treatment of aquaculture effluents-what can we learn from the past for the future? *Sustainability-Basel* 6, 836–856. doi: 10.3390/su6020836

van Rijn, J. (2013). Waste treatment in recirculating aquaculture systems. *Aquacult Eng.* 53, 49–56. doi: 10.1016/j.aquaeng.2012.11.010

Verdegem, M. C. J. (2013). Nutrient discharge from aquaculture operations in function of system design and production environment. *Rev. Aquacult* 5, 158–171. doi: 10.1111/raq.12011

Wang, J. J., Beusen, A. H. W., Liu, X. C., and Bouwman, A. F. (2020). Aquaculture production is a large, spatially concentrated source of nutrients in chinese freshwater and coastal seas. *Environ. Sci. Technol.* 54, 1464–1474. doi: 10.1021/acs.est.9b03340

Wang, B. D., Xin, M., Wei, Q. S., and Xie, L. P. (2018). A historical overview of coastal eutrophication in the China Seas. *Mar. Pollut. Bull.* 136, 394–400. doi: 10.1016/j.marpolbul.2018.09.044

Wu, T. T., Bi, F., Liu, H. T., Wang, S. Q., He, P. M., and Zhang, J. H. (2025a). Identification of nitrogen-fixing bacteria on green tide-causing species and evaluation of their nitrogen-fixing capacity. *Bioresource Technol.* 428, 132450. doi: 10.1016/j.biortech.2025.132450

Wu, T. T., Liu, W., Liu, J. F., Sun, J. Y., Liu, H. T., Qin, Y. T., et al. (2025b). Nutrient-driven biomass variation in *Ulva prolifera*: Experimental insights for predicting Yellow Sea green tide magnitude. *Algal Res.* 90, 104143. doi: 10.1016/j.algal.2025.104143

Xia, Z. Y., Liu, J. L., Zhao, S., Sun, Y. Q., Cui, Q. W., Wu, L. J., et al. (2024). Review of the development of the green tide and the process of control in the southern Yellow Sea in 2022. *Estuar. Coast. Shelf S* 302, 108772. doi: 10.1016/j.ecss.2024.108772

Xiu, B., Liang, S. K., He, X. L., Wang, X. K., Cui, Z. G., and Jiang, Z. J. (2019). Bioavailability of dissolved organic nitrogen and its uptake by *Ulva prolifera*: Implications in the outbreak of a green bloom off the coast of Qingdao, China. *Mar. Pollut. Bull.* 140, 563–572. doi: 10.1016/j.marpolbul.2019.01.057

Xu, N., Xu, K., Xu, Y., Ji, D., Wang, W., and Xie, C. (2024). Interactions between nitrogen and phosphorus modulate the food quality of the marine crop *Pyropia haitanensis* (TJ Chang & BF Zheng) N. *Kikuchi M. Miyata (Porphyra haitanensis). Food Chem.* 448, 138973. doi: 10.1016/j.foodchem.2024.138973

Yan, H. F., Kyne, P. M., Jabado, R. W., Leeney, R. H., Davidson, L. N. K., Derrick, D. H., et al. (2021). Overfishing and habitat loss drives range contraction of iconic marine fishes to near extinction. *Sci. Adv.* 7, abb6026. doi: 10.1126/sciadv.abb6026

Zhang, Y. Y., He, P. M., Li, H. M., Li, G., Liu, J. H., Jiao, F. L., et al. (2019). Ulva prolifera green-tide outbreaks and their environmental impact in the Yellow Sea, China. *Natl. Sci. Rev.* 6, 825–838. doi: 10.1093/nsr/nwz026

Zhang, P. Y., Xin, Y., Zhong, X. S., Yan, Z. W., Jin, Y. M., Yan, M. J., et al. (2021). Integrated effects of *Ulva prolifera* bloom and decay on nutrients inventory and cycling in marginal sea of China. *Chemosphere* 264, 128389. doi: 10.1016/j.chemosphere.2020.128389